RSC Advances




ROYAL SOCIETY OF CHEMISTRY

www.rsc.org/advances

RSC advances

PAPER

View Article Online

View Journal | View Issue

# Selective extraction of metallic arc-discharged single-walled carbon nanotubes by a water soluble polymethylsilane derivative

Received 00th January 20xx,
Accepted 00th January 20xx

DOI: 10.1039/x0xx00000x

www.rsc.org/

Jinling Gao[a,b], Yao Huang[a], Yongfu Lian[a,*]

Water soluble polymethyl(1-undecylic acidyl)silane, synthesized by the hydrosilylation of 10-undecylenic acid with polymethylsilane catalyzed by 2,2'-azobisisbutyronitrile, demonstrates selective extracting ability toward metallic single-walled carbon nanotubes (SWNTs) produced by arc discharge method. After heating in air at a temperature of 673 K and treatment with concentrated hydrochloric acid, the arc-discharged SWNTs are ultrasonically dispersed in an aqueous solution of polymethyl(1-undecylic acidyl)silane. Such obtained dispersions are subjected to ultracentrifugation, and then the supernatants are collected. Optical absorption spectra show that the supernatants enrich in metallic SWNTs. Moreover, Raman spectra confirm the selective extraction of *(14,2)*, *(15,0)*, (*13,1*), *(12,3)* and *(19,1)* metallic SWNTs, which are of larger diameters and smaller chiral angles than those reported previously. Additionally, FT-IR spectroscopy and Raman scattering evidence the charge transfer between polymethyl(1-undecylic acidyl)silane and SWNTs. It is conjectured that polymethyl(1-undecylic acidyl)silane could chiral-index-selective wrap onto SWNTs through a fairly weak CH-π interaction. Thus, we believe that the stiffness and length of main chains and side chains as well as the charge state of the polymethylsilane derivative play vital roles in the selective extraction of SWNTs.

## 1. Introduction

Single-walled carbon nanotubes (SWNTs) have attracted considerable attentions because of their unique electrical, mechanical, thermal and optical properties, which are significant to all kinds of potential technological applications.[1–9] Usually, as-synthesized SWNTs usually form large bundles containing many kinds of species. In order to get better performance of materials, people have dispersed as-synthesized SWNTs samples in many solubilizing agents and separated them in line with their length, diameter, metallicity, (*n*, *m*) structure and handedness by electrophoresis,[10,11] centrifugation,[12-14] chromatography,[15-20] selective solubilization[21-24] and selective reaction.[25-27]

Normally, SWNTs are solubilized or individually dispersed either by covalent chemical functionalization or by non-covalent dispersion with the assistance of biological macromolecules, surfactants, ionic liquids and polymers.[28-30] Among the polymers applied, nonaromatic polyvinylpyrrolidone, polystyrenesulfonate, poly(allylamine) and α-helical amphiphilic peptides show dispersing ability to SWNTs in aqueous media, and semiconducting SWNTs are selectively extracted out.[31-33] On the other hand, $\pi$-conjugated polymers Particularly polyfluorene (PFO) homo- and co-polymers are evidenced to be able to selectively extract specific semiconducting SWNTs.[34] It should be noted that PFO itself show effective interactions only with smaller diameter SWNTs (0.8–1.2 nm), and poly(dialkylfluorene)s with increasing lengths of alkyl chains can interact with nanotubes of larger diameter up to 1.5 nm.[35] Moreover, poly[dioctylfluorene)-alt-(benzo-thiadiazole) (F8BT) and copolymer of dioctylfluorene and bipyridine units (PFO-BPy) demonstrate selective extraction towards semicnducting SWNTs with specific chiral indexes of (*15*, *4*)[36] and (*6*, *5*),[37] respectively. Meanwhile, poly-[di(N,N-dimethylaminopropyl)fluorene] (PFDMA) and poly[di(N,N,N-trimethylammoniumpropyl)fluorene dibromide] (PFAB) are proved to be able to selectively extract semiconducting (*6*, *5*) and (*7*, *5*) SWNTs.[38] Recently, it is found that copolymers composed of fluorene or aryleneethynylene and chiral binaphthol units exhibit judicious separation of left- and right-handed semiconducting SWNTs.[39,40] Additionally, regioregular poly(3-alkylthiophene)s (rr-P3ATs) including rr-P3DT (alkyl = n-decyl) and rr-P3DDT (alkyl = ndodecyl) are reported to be also applicable to the selective extraction of semiconducting HiPCO and CoMoCAT nanotubes.[41]

Polysilane is a typical nonaromatic σ-conjugated polymer, composed of alkyl side chains attached to the silicon-catenated main chain. From a view point of electronic structure, polysilane can be regarded as a quasi-one-dimensional material, due to the delocalized σ- conjugated electrons along the Si main chain.[42,43] Naito *et al* reported the solubilization of CoMoCAT SWNTs in THF by a series of poly(dialkylsilane).[44,45] It is found that the polysilanes bearing methyl and n-alkyl side chains are able to solubilize

[a] Key Laboratory of Functional Inorganic Material Chemistry, Ministry of Education, School of Chemistry and Materials Science, Heilongjiang University, Harbin 150080, China.
[b] Collage of science,Heilongjiang Bayi Agricultural University,Daqing,163319, China.
*corresponding author: Professor Yongfu Lian, e-mail: chyflian@hlju.edu.cn
Electronic Supplementary Information (ESI) available: additional the synthesis of polymethylsilane, vis-NIR, SEM, TEM (S1-S4). See DOI:10.1039/x0xx00000x

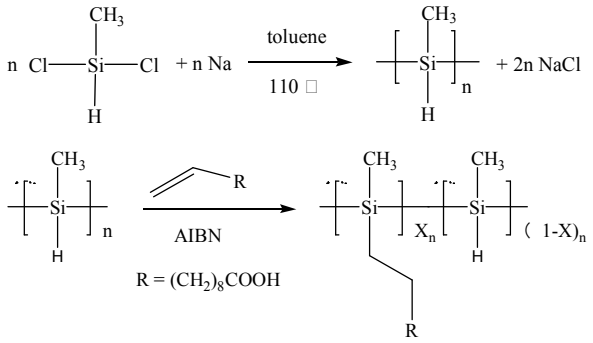


**Scheme 1.** Preparation of water soluble polymethyl(1-undecylic acidyl)silane.

CoMoCAT SWNTs in THF, resulting in the enrichment of semiconducting (7,6) and (9,4) SWNTs with ca. 0.9 nm on diameter.

SWNTs can be produced in large quantities by arc discharge,[46] chemical vapor deposition,[47] laser ablation,[48] the CoMoCAT process,[49] and high-pressure carbon monoxide disproportionation (HiPCO).[50] All these processes yield mixtures of semiconducting and metallic SWNTs with variations in the distribution of the (*n,m*) indices within certain diameter ranges. CoMoCAT and HiPCO SWNTs are largely employed to the formation of stable dispersion of SWNTs. They are formed at a temperature ca. 1273 K and with diameters distributed from 0.7 to 1.2 nm. Whereas, arc-discharged SWNTs are generated at a temperature higher than the evaporating point of graphite, and this process yields a random distribution of metallic and semiconducting SWNTs with diameter ranging from 0.8 to 2.0 nm. In comparison with the others, arc-discharged SWNTs are longer and straighter with fewer defects and usually tend to form large bundles due to the stronger van der Waals interaction, which make them more difficult to be solubilized.[51] Up to the present, there are no reports on the selective solubilization of arc-discharged SWNTs with polymers, neither in line with their length, diameter, metallicity, (*n*, *m*) structure nor handedness

In this study, a water soluble polymethylsilane derivative (scheme 1) is firstly applied to the selective extraction of SWNTs. Optical absorption spectroscopy, Raman spectroscopy confirm the selective extraction of metallic arc-discharged SWNTs. Moreover, those metallic SWNTs are largely enriched, indicating the first successful isolation of metallic SWNTs with large diameters and small chiral angles.

## 2. Experimental

### 2.1 Preparation and purification of SWNTs

As-synthesized SWNTs were prepared by an improved arc discharge procedure.[46] The anode was an Ø6 x 120 mm specpure graphite rod drilled with an Ø4 x 100 mm hole and filled with a powdered mixture of graphite and catalysts including Y-Ni alloy and Fe-S compound. The cathode was a 40 x 40 mm graphite block. An arc was generated with an electric current of 100 A under a helium atmosphere of 500 Torr. After cooling down, as synthesized SWNTs were collected from the arc discharge chamber.

The as synthesized SWNTs were thermally treated at 673 k for 3 h in an air atmosphere to burn out amorphous carbons, and then soaked in concentrated hydrochloric acid for 24 h to remove metal catalysts. After washed with a large amount of water and dried, the product was supersonically dispersed in 1% (wt/v) aqueous sodium deoxycholate solution. Such obtained dispersion was subjected to centrifugation at rotation speed of 15,000 rpm for 2 h at 10 ℃, and the above 80% supernatants were collected (named DOC-SWNTs).

### 2.2. Synthesis of polymethyl(1-undecylic acidyl)silane

The water soluble polymethyl(1-undecylic acidyl)silane, was synthesized by the following two steps (Scheme 1). Polymethylsilane was firstly prepared by a sodium-mediated Wurtz reductive coupling of dichloromethylsilane in refluxing toluene.[43] Secondly, polymethyl(1-undecylic acidyl)silane was synthesized by the hydrosilylation of 10-undecylenic acid with polymethylsilane using 2,2'-azobisisbutyronitrile (AIBN) as initiator.[52] 4.4 g polymethylsilane (containing 0.1 mol Si-H) and 0.4 g 2,2'-azobisisbutyronitrile were dissolved into 80 ml THF in a three-necked flask. After dissolved into 20 ml THF, 18.4 g 10-undecylenic acid（0.1 mol）was added drop by drop at the reflux temperature of THF under the aegis of the highly pure nitrogen. The reactant mixture was refluxed for 12 h at 68 ℃, and then filtered with normal filter paper. The filtrate was evaporated with a rotary evaporator to remove THF solvent, and then extracted with hexane and separated with a separating funnel for several times to get purified product. Such prepared polymethyl(1-undecylic acidyl)silane is a yellow viscous liquid, soluble in alkaline water, toluene, THF and ethanol.

### 2.3 Selective extraction and isolation of SWNTs

In a typical experiment, 10 mg HCl-treated SWNTs were ultrasonically (Sonics, VCX 750, Vibra-cell, USA) dispersed in 100 ml alkaline aqueous solution of polymethy(1-undecylic acidyl)silane 1% (wt/v) (pH = 8) for 12 h at a temperature of 10 ℃. The resulting dispersion was then centrifuged with an angle rotor (P70AT2, CP70MX, Hitachi KokiCo.) at a rotation speed of 15000 rpm for 2 h, and the above 80% supernatants were carefully collected. After evaporation with a rotary evaporator, the complex of polymethy(1-undecylic acidyl)silane and SWNTs was obtained.

### 2.4 Characterization methods

2.4.1 The vis-NIR optical adsorption spectra were recorded by a computer manipulated dual-beam spectrometer (UV3600, Shimadzu) with a 10 mm quartz cell and a spectral resolution of 0.2 nm.

2.4.2 The Fourier transform-infrared (FT-IR) spectra were recorded on Fourier transform infrared spectroscopy (Spectrum one, PerkinElmer). The samples were prepared by dropping polymethylsilane, polymethyl(1-undecylic acidyl)silane and the DMF solution of the complex of polymethyl(1-undecylic acidyl)silane and SWNTs onto KBr pellets with capillary and measured in transmittance mode.

2.4.3 The scanning electron microscopy (SEM) images of the complex of polymethyl(1-undecylic acidyl)silane and SWNTs



 

dispersions were taken on a cold field emission scanning microscope (S4800, Hitachi) operated at an acceleration voltage of 5.0 kV. The complex of polymethyl(1-undecylic acidyl)silane and SWNTs was drop-casted on silicon substrate and sputter-coated with a thin layer of Au.

2.4.4 Raman spectroscopy at room temperature was recorded by a micro laser Raman spectrometer (HR800, Jobin Yvon) under excitation at 488, 514, 633, and 785 nm, respectively. The samples were prepared by filtering the centrifugates of DOC-SWNTs and the complex of polymethyl(1-undecylic acidyl)silane and SWNTs with 0.1 $\mu$m PTFE microfilm and subsequently dried for 1 day in a vacuum at 150 °C, respectively. A 100× air objective was used, and the laser spot was about 1 μm in diameter. The laser power was carefully controlled to avoid any heating effect on Raman shifts.

2.4.5 Atomic force microscope (AFM) observations were performed on an AFM/SPM system (SPM 5100, Agilent). Samples were prepared by casting one drop of the complex of polymethyl(1-undecylic acidyl)silane and SWNTs and dried on a freshly cleaved mica substrate and observed in the tapping-mode of operation.

## 3. Results and discussion

### 3.1. The Formation of polymethyl(1-undecylic acidyl)silane

Shown in Fig. 1 are the FT-IR spectra of Polymethylsilane, 10-undecylenic acid, and polymethyl(1-undecylic acidyl)silane. The absorption band of 2100 $cm^{-1}$ observed in Fig. 1a is assigned to the stretching vibration of Si-H bond, the characteristic IR absorption band of polymethylsilane, and the absorption band of 1620 $cm^{-1}$ observed in Fig. 1b is ascribed to the stretching vibration of C=C bond. It can be seen from Fig. 1c that the characteristic IR absorption band of polymethylsilane is significantly softened in comparison with that in Fig. 1a. Whereas, the stretching vibration band of C=C bond is completely disappeared. Thus, it is concluded that the hydrosilylation of 10-undecylenic acid with polymethylsilane occurs between the SI-H bonds in polymethylsilaneand the C=C bond in 10-undecenoic acid, and that the side chain of 10-undecylenic acid is attached to the main chain of polymethylsilane through anti-Markovnikov addition reaction. With the formation of polymethyl(1-undecylic acidyl)silane, the molecular chain of polymethylsilane is unfolded,[42] and the cross-linking reactions among Si-H bond are hindered. Particularly, the hydrophilic -COOH groups in the side chain make the polymethylsilane derivative soluble in water.

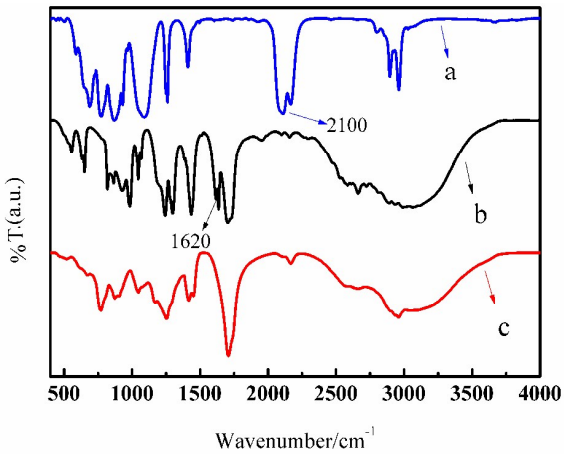


Fig. 1 FT-IR spectra of polymethylsilane (a)，10-undecylenic acid (b)，and polymethyl(1-undecylic acidyl)silane (c).

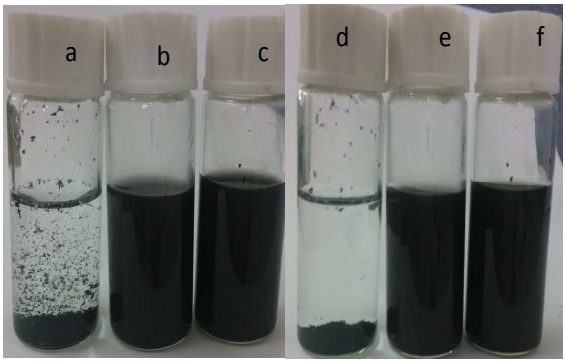


Fig. 2 The photographs of SWNTs dispersed in water (a), the aqueous solutions of polymethyl(1-undecylic acidyl)silane (b), and the aqueous solutions of DOC (c). (d), (e) and (f) are taken after (a), (b) and (c) setting for 30 days, respectively.

### 3.2. The disperse ability of polymethyl(1-undecylic acidyl)silane towards SWNTs

Fig. 2 demonstrates the photographs of SWNTs dispersed in water, the aqueous solutions of polymethyl(1-undecylic acidyl)silane, and the aqueous solutions of DOC. It can be seen from Figs. 2b&2c that black dispersions of SWNTs are formed with the assistance of polymethyl(1-undecylic acidyl)silane and DOC, respectively. In sharp contrast, some fine black particles are visible in Fig. 2a. After setting for 30 days, the dispersions of SWNTs with the polymethyl(1-undecylic acidyl)silane and DOC show a much strong stability (see Figs. 2e&2f). Whereas the SWNTs dispersed in water undergo serious agglomeration and precipitate completely. It is obvious that polymethyl(1-undecylic acidyl)silane demonstrates a similar disperse ability towards SWNTs to that of DOC.

Microstructural characterization of the complex of polymethyl(1-undecylic acidyl)silane and SWNTs was performed using AFM. The typical AFM images of the complex of polymethyl(1-undecylic acidyl)silane and SWNTs (Fig. 3), clearly shows the presence of many long filamentous structures. These structures are ascribed to the complex of polymethyl(1-undecylic acidyl)silane and SWNTs, in which very straight SWNTs are observed with an average length about 1.8 μm. The dome-like structures observed on the substrate are considered to be composed of molecular aggregates of polymethyl(1-undecylic acidyl)silane, which is consisted of three distinct parts, i.e. horizontally self-assembled monolayer (0.8 nm), transition state (2 nm) and vertically alignment (8.0 nm).[53,54]

From Fig. 3, it can be seen that the complexes of SWNTs and polymethyl(1-undecylic acidyl)silane coexist with free polymethyl(1-undecylic acidyl)silane in the supernatant. Moreover, SWNTs are

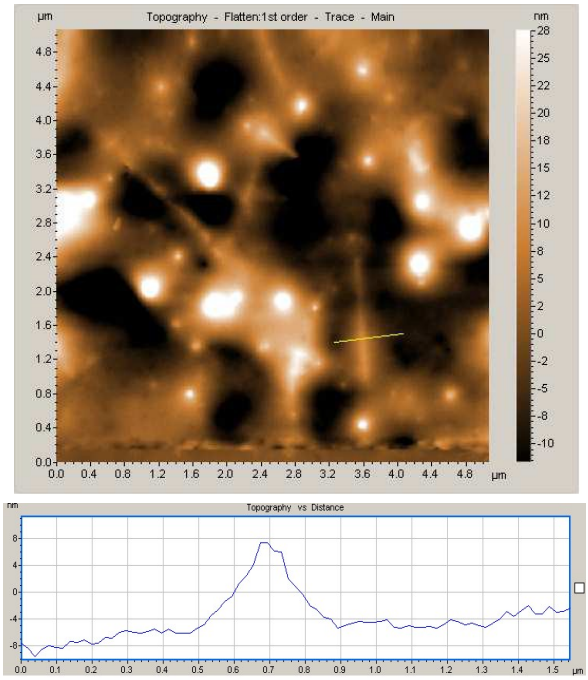


Fig. 3 AFM images of the complex of polymethyl(1-undecylic acidyl)silane and SWNTs.

observed to be well coated by polymethyl(1-undecylic acidyl)silane with varying thickness, and to be well dispersed. Height analysis in different regions (indicated by white solid lines in the image) produced values ranging from 6 to 10 nm. Considering the varying orientation of the polysilane derivative and the varying thickness of the coating on SWNTs, it is reasonable for us to assign the SWNTs observed here as individual ones. Therefore, the AFM image evidences that polymethyl(1-undecylic acidyl)silane strongly interacts with SWNTs and is able to exfoliate them into individual ones or very small bundles in water, leading to the good dispersing ability of polymethyl(1-undecylic acidyl)silane towards SWNTs.

To provide further support for the good dispersing ability of polymethyl(1-undecylic acidyl)silane towards SWNTs, SEM observation was carried out. Shown in Fig. 4 is the SEM image of the complex of polymethyl(1-undecylic acidyl)silane and SWNTs dropped and dried on Si wafer. Because of the bad electronic conductivity of polymethyl(1-undecylic acidyl)silane unevenly coated on SWNTs, the SEM image of the complex is usually not as clear as those of naked SWNTs. It is obvious that small bundles of SWNTs are observed to be coated with blurred materials and branch cross-linked to some extent. It is no doubt that these blurred materials are self-assembled polymethyl(1-undecylic acidyl)silane, indicating that they are wrapped onto the surface of carbon nanotubes. The branch cross-linked appearance is assumed to be formed from these well dispersed individual or thin bundles of SWNTs. During the preparation of SEM samples, they aggregate to

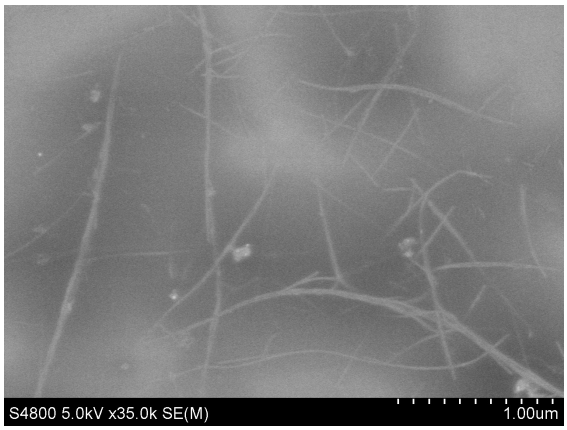


Fig. 4 The SEM image of the complex of polymethyl(1-undecylic acidyl)silane and SWNTs.

larger bundles under the driving of the self-assembly of polymethyl(1-undecylic acidyl)silane, being observed as rigid structures.

Additionally, the SEM image shown in Fig. 4 is recorded with the SWNTs freshly dispersed in the aqueous solutions of polymethyl(1-undecylic acidyl)silane (see Fig. 2b). After the SWNTs freshly dispersed in the aqueous solutions of polymethyl(1-undecylic acidyl)silane setting for 30 days, the diameter of SWNTs bundles increases to as large as 120 to 250 nm (see Fig. S2). It is estimated that such strong self-assembly would influence its selective dispersing ability toward SWNTs to some extent.

### 3.3 The selective extraction of metallic SWNTs

UV-vis-NIR spectroscopy is sensitive to the presence of metallic and semiconducting SWNTs. Shown in Fig. 5 are the vis-NIR absorption spectra of DOC-SWNTs (a), and the complex of SWNTs and polymethyl(1-undecylic acidyl)silane (b), solubilized in water. In order to avoid the disturbance from water absorption, the vis-NIR absorption spectra are recorded in the wavelength range from 400 to 1400 nm. For arc-discharged SWNTs, the absorption bands in the 600-800, 850-1290 nm regions are attributed to the first van Hove transition of metallic SWNTs ($M_{11}$), and the second van Hove transition of semiconducting SWNTs ($S_{22}$). It could be seen from Fig. 5 that the absorption curve b demonstrates more fine features than curve a, resulting from the better dispersing ability of polymethyl(1-undecylic acidyl)silane towards SWNTs than that of DOC. As a matter of fact, the distinguishable and intense peaks in Fig. 5b indicate that the arc-discharged SWNTs are individually solubilized in the aqueous solution of polymethyl(1-undecylic acidyl)silane. Though DOC is a good agent for the solubilization of SWNTs, it does not show any selectivity for a special kind of carbon nanotubes. Therefore DOC-SWNTs is a good contrasting object for the evaluation of the selective extraction of polymethyl(1-undecylic acidyl)silane towards SWNTs. As illustrated in Fig. 5, the band area in the $M_{11}$

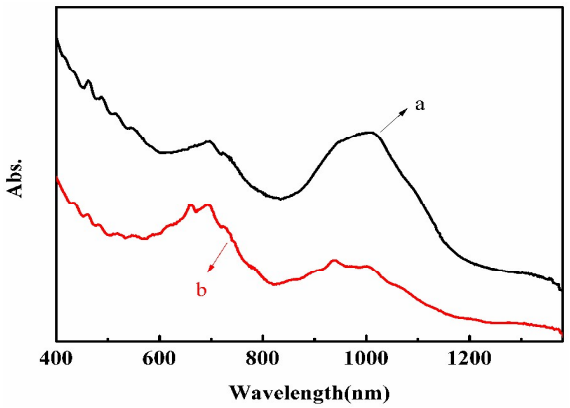


Fig.5 The normalized vis-NIR spectra of DOC-SWNTs (a), and the complex of polymethyl(1-undecylic acidyl)silane and SWNTs (b).

region increases from curve a to curve b, whereas the band area in the $S_{22}$ region decreases in the same order. It appears that polymethyl(1-undecylic acidyl)silane preferentially extracts metallic SWNTs, leading to the supernatants enriched in metallic species and suppressed in semiconducting ones. Moreover, it is also observed that the average absorption is blue-shifted from curve a to curve b for both the $M_{11}$ band and the $S_{22}$ band. We speculate that such blue shift is owing to the selective extraction of polymethyl(1-undecylic acidyl)silane towards SWNTs with varying diameters or even with varying (*n,m*) structures.

An estimate of the relative abundance of metallic or semiconducting SWNTs can be derived by integrating the peak areas in the $M_{11}$ and $S_{22}$ regions in line with the method proposed by Haddon et al.[55] As show in Fig. 6, in the $M_{11}$ region the ratios of the areas under the curves after and before baseline subtraction, AA(S)/AA(T) are 0.060 and 0.154 for DOC-SWNTs and for the complex of polymethyl(1-undecylic acidyl)silane and SWNTs, respectively. Therefore, the relative carbonaceous purity of the metallic SWNTs in complex of SWNTs and polymethyl(1-undecylic acidyl)silane to that in DOC-SWNTs is about 2.567 (0.154/0.060). Similarly, in the $S_{22}$ region the ratios of the areas under the curves after and before baseline subtraction, AA(S)/AA(T) are 0.191 and 0.138 for DOC-SWNTs and for the complex of polymethyl(1-undecylic acidyl)silane and SWNTs, respectively. Therefore, the relative carbonaceous purity of the semiconducting SWNTs in complex of SWNTs and polymethyl(1-undecylic acidyl)silane to that in DOC-SWNTs is about 0.723 (0.138/0.191). Thus，the content of metallic SWNTs in the complex of polymethyl(1-undecylic acidyl)silane and SWNTs is about 3.55 (2.567/0.723) times of that of semiconducting ones, highlighting the selective extracting ability of polymethyl(1-undecylic acidyl)silane towards metallic SWNTs.

It is well known that Raman spectroscopy is a powerful technique to characterize carbon materials. To further investigate the special selectivity of polymethyl(1-undecylic acidyl)silane towards metallic SWNTs, resonant Raman spectroscopy was applied under excitation at 488, 514, 633, and 785 nm, respectively, which will bring varying metallic and semiconducting arc-discharged SWNTs into resonant scattering. The energy of the species interband electronic transition

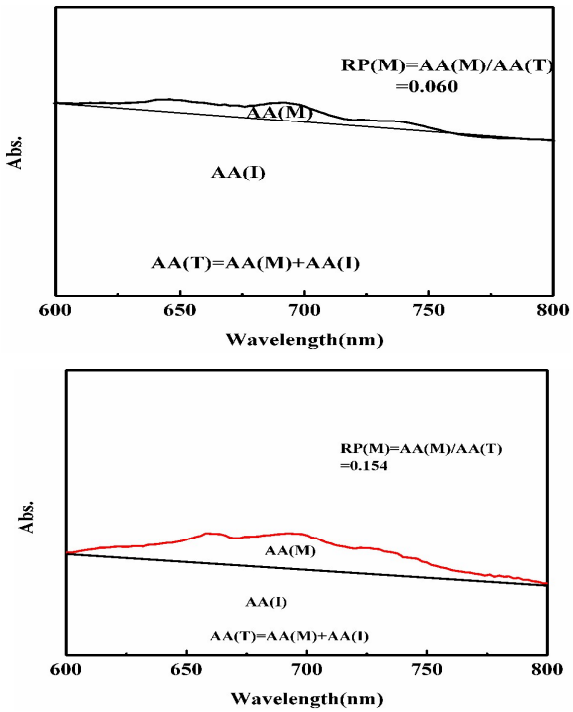


**Fig. 6** The relative purity of DOC-SWNTs (upper) and the complex of polymethyl(1-undecylic acidyl)silane and SWNTs (lower) based on the vis-NIR absorption spectra.

depends on the diameter and metallicity of SWNTs, and the diameters of SWNTs are inversely proportional to radial breathing modes (RBM) peaks in the 100-400 $cm^{-1}$ range.

Shown in Fig. 7 are the normalized Raman spectra of DOC-SWNTs and the complex of polymethyl(1-undecylic acidyl)silane and SWNTs under excitation at 488, 514, 633, and 785 nm, respectively. The Raman spectra are normalized at the G+ band (around 1590 $cm^{-1}$). According to the reference Kataura plot and the wavelength of excitation laser, the RBM peaks in these Raman spectra are assigned to SWNTs species. In the 633 nm excitation spectrum (Fig. 7a), the RBM peaks appeared in the wave number range of 154-201 $cm^{-1}$ are due to metallic SWNTs and those appeared in the wave number range of 201-240 $cm^{-1}$ own to semiconducting ones. It can be seen that the DOC-SWNTs show two peaks in the wavenumber range of 154-201 $cm^{-1}$ (173 $cm^{-1}$ and 189 $cm^{-1}$) and one prominent peak in the range of 201-240 $cm^{-1}$ (216 $cm^{-1}$), assignable to carbon nanotubes with indices of (*14,2*), (*15,0*) and (*11,1*), respectively. Whereas the complex of polymethyl(1-undecylic acidyl)silane and SWNTs only show two strong peaks in the wavenumber range of 154-201 $cm^{-1}$ (169 $cm^{-1}$ and 185 $cm^{-1}$) assigned to carbon nanotubes with indices of (*14,2*) and (*15,0*), and no discernable peaks are observed in the range of 201-240 $cm^{-1}$. Fig. 7c shows the Raman RBM spectra with 488 nm excitation. The peaks from 194 to 221 $cm^{-1}$ are ascribed to metallic and those from 140 to 194 $cm^{-1}$ to semiconducting SWNTs. It can be seen that the DOC-SWNTs show one prominent peak in the range of 140-194 $cm^{-1}$ (180 $cm^{-1}$),

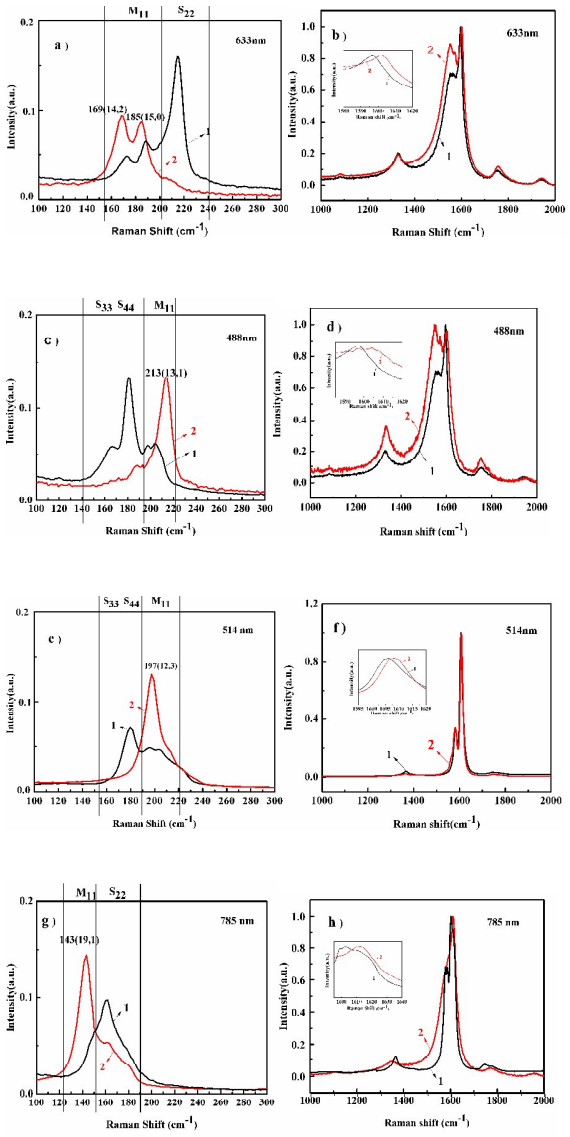


Fig. 7 Raman spectra of DOC-SWNTs (1) and the complex of polymethyl(1-undecylic acidyl)silane and SWNTs (2 ) in the ranges of 100 - 300 $cm^{-1}$ ( a, c, e, g ) and 1000 - 2000 $cm^{-1}$ ( b, d, f, h ), respectively.

assignable to carbon nanotubes with indices of (*15,4*). Whereas the complex of polymethyl(1-undecylic acidyl)silane and SWNTs show one strong peaks in the wavenumber range of 194-221 $cm^{-1}$ (213 $cm^{-1}$) assigned to carbon nanotubes with indices of (*13,1*). Fig. 7e shows the Raman RBM spectra with 514 nm excitation. The peaks from 189 to 221 $cm^{-1}$ are ascribed to metallic and those from 152 to 189 $cm^{-1}$ to semiconducting SWNTs. It can be seen that the DOC-SWNTs show one prominent peak in the range of 152-189 $cm^{-1}$ (179 $cm^{-1}$), assignable to carbon nanotubes with indices of (*11,9*). Whereas the complex of polymethyl(1-undecylic acidyl)silane and SWNTs show one strong peaks in the wavenumber range of 189-221 $cm^{-1}$ (197 $cm^{-1}$) assigned to carbon nanotubes with indices of

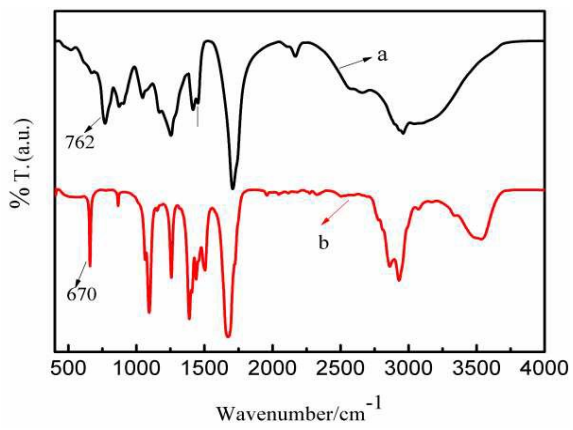


Fig.8 FT-IR spectra of polymethyl(1-undecylic acidyl)silane (a) and the complex of polymethyl(1-undecylic acidyl)silane-SWNTs (b).

(*12,3*). Fig. 7g shows the Raman RBM spectra with 785 nm excitation. The peaks from 122 to 151 $cm^{-1}$ are ascribed to metallic and those from 151 to 190 $cm^{-1}$ to semiconducting SWNTs. It can be seen that the DOC-SWNTs show one prominent peak in the range of 151-190 $cm^{-1}$ (161 $cm^{-1}$), assignable to carbon nanotubes with indices of (*13,3*). Whereas the complex of polymethyl(1-undecylic acidyl)silane and SWNTs show one strong peaks in the wavenumber range of 122-151 $cm^{-1}$ (143 $cm^{-1}$) assigned to carbon nanotubes with indices of (*19,1*). The polymethyl(1-undecylic acidyl)silane shows selectively extracting ability toward metallic carbon nanotubes with indices of (*14,2*), (*15,0*) with 633 nm excitation, (*13,1*), (12,3), (19,1) with 488 nm, 514 nm and 785 nm excitation, respectively. Therefore, it is concluded that polymethyl(1-undecylic acidyl)silane could selectively extract metallic carbon nanotubes and discriminate semiconducting species, in consistent with the results out of vis-NIR characterization.

The G band of SWNTs is actually composed of double peaks, i.e., the lower broad G- band (1520-1560 $cm^{-1}$) and the upper sharp G+ band (around 1590 $cm^{-1}$). According to Yi et al, G- and G+ bands indicate the presence of metallic and semiconducting SWNTs, respectively,[56] and the metallic SWNTs normally show the asymmetric and wider Breit-Wigner-Fano (BWF) satellite band close to the upper *G* band.[57] It can be seen from Fig. 7 (b, d, f, h) that the G- band of the complex of polymethyl(1-undecylic acidyl)silane and SWNTs widens because of elevated intensity relative to that of DOC-SWNTs. From the viewpoint of metallicity, the wider and more pronounced BWF feature means that the complex of polymethyl(1-undecylic acidyl)silane and SWNTs enriches in metallic species, evidencing the special selectivity of polymethyl(1-undecylic acidyl)silane towards metallic SWNTs.

### 3.4 Formation of the electron donor-acceptor complex between polymethyl(1-undecylic acidyl)silane and metallic-SWNTs

FT-IR spectroscopy is applied to the investigation on the charge transfer between polymethyl(1-undecylic acidyl)silane and SWNTs. Shown in Fig. 8 are the FT-IR spectra of polymethyl(1-undecylic

acidyl)silane and the polymethyl(1-undecylic acidyl)silane-SWNTs complex. It can be seen that the Si-C characteristic absorption peak red-shifts from 762 $cm^{-1}$ in polymethyl(1-undecylic acidyl)silane sample to 670 $cm^{-1}$ in the polymethyl(1-undecylic acidyl)silane-SWNTs complex. The weakness of Si-C bonds is ascribed to a result of the charge transfer from the SWNTs to the partial occupation of the low lying antibonding acceptor orbital[58] of polymethyl(1-undecylic acidyl)silane. Additionally，in comparison with those observed for polymethyl(1-undecylic acidyl)silane the other FT-IR characteristic features are also red-shifted, because of the charge transfer in the polymethyl(1-undecylic acidyl)silane-SWNTs complex.

Moreover, Raman spectroscopy could probe the impact of charge transfer on the electronic structures of the doped SWNTs. According to Wise et al,[58] removing charge from SWNTs would result in an upshift in the G+ band peak around 1592 $cm^{-1}$, while adding charge to SWNTs results in a downshift. It can be seen from the inset of Fig. 7 (b, d, f, h) that the G+ band is upshifted to 1596 $cm^{-1}$, 1597$cm^{-1}$, 1604$cm^{-1}$, 1604$cm^{-1}$ for DOC-SWNTs and to 1601 $cm^{-1}$, 1604$cm^{-1}$, 1609$cm^{-1}$, 1610$cm^{-1}$ for the polymethyl(1-undecylic acidyl)silane-SWNTs complex. Obviously, the upshift in the G+ band peak is a result of the charge transfers from SWNTs to DOC or to polymethyl(1-undecylic acidyl)silane. The larger the upshift in the G+ band peak indicates the more the charge transferred. Therefore, it is concluded that more charge is transferred to polymethyl(1-undecylic acidyl)silane than to DOC from SWNTs.

The experimentally derived work function, the negative of the Fermi level, is 4.8-5.0 eV for metallic or small band gap semiconducting SWNTs.[59,60] There are some free electrons at the Fermi levels of metallic SWNTs, whereas the electrons are bounded in the low lying valence band for semiconducting ones. Thus, the charge transfer from metallic SWNTs to polymethyl(1-undecylic acidyl)silane is more efficient than that from semiconducting counterpart, leading to the successful formation of the complex between polymethyl(1-undecylic acidyl)silane and metallic SWNTs. The selective extraction of metallic SWNTs with polymethyl(1-undecylic acidyl)silane is a result of the formation of their electron donor-acceptor complex.

Naito et al[44,45] investigated the polymer wrapping behaviors of poly(dialkylsilane)s around SWNTs, and concluded that the stiffness and conformation played an essential role in the wrapping of poly(disilane)s onto SWNTs. As a matter of fact, the stiffness and conformation of poly(dialkylsilane)s are largely decided by the alkyl side chains. The dome-like structures observed in Fig. 3 reflect that the random-coiled polymethyl(1-undecylic acidyl)silane is flexible,[61] and it is reasonable to assume that polymethyl(1-undecylic acidyl)silane is successfully wrapped onto the arc-discharged SWNTs to form a stable complex. After wrapping the plane of dihedral angel of Si main chain placed almost perpendicular to the grapheme surface of SWNTs, with its sides chains (methyl and 1-undecylic acidyl) adopting nearly all-trans zigzag conformation to fit the surface curvatures of the SWNTs. Such geometric distortion of polymethyl(1-undecylic acidyl)silane should play a crucial role for stabilizing its electron donor-acceptor complex with SWNTs.

From Fig. 8 it can be observed that the stretching bands of $CH_2$ and $CH_3$ at 2800-3100 $cm^{-1}$ are downshifted 12-15 $cm^{-1}$, indicating the existence of CH-$\pi$ interactions[62] among the linear alkyl side chains of polymethyl(1-undecylic acidyl)silane and the curved grapheme surface of SWNTs.[45] If the main Si chain and the linear side chains of polymethyl(1-undecylic acidyl)silane are aligned respectively in the axial and radial directions of SWNTs, the side chains methyl and 1-undecylic acidyl might form a circle tightly attached onto SWNTs through the above CH-$\pi$ interactions. In this situation, the diameter of such formed circle ought to match those of wrapped SWNTs to some extent. Therefore, the length of the linear side chains of polymethyl(1-undecylic acidyl)silane endows selective wrapping for SWNTs with specific diameters.

## Conclusion

A water soluble polymethylsilane derivative, polymethyl(1-undecylic acidyl)silane, is synthesized by the hydrosilylation of 10-undecylenic acid. Spectroscopic characterizations by vis-NIR and Raman confirm that polymethyl(1-undecylic acidyl)silane displays selective extraction towards arc-discharged metallic SWNTs through a simple sonication and centrifugation process. FT-IR and Raman spectra prove the charge transfer from metallic SWNTs to polymethyl(1-undecylic acidyl)silane, leading to the formation of the donor-acceptor complex between polymethyl(1-undecylic acidyl)silane and metallic SWNTs. Moreover, the side chains of polymethyl(1-undecylic acidyl)silane are wrapped onto SWNTs by the accumulation of multiple CH-π interactions. The diameters of the extracted SWNTs are correlated with the lengths of side chains (methyl and 1-undecylic acidyl). Thus, larger diameters and small chiral angles metallic SWNTs are selectively extracted by polymethyl(1-undecylic acidyl)silane.

It is expected that the polymethyl(1-undecylic acidyl)silane closely wrapped metallic SWNTs might be a good electronic cable for nanodevices, and they could also be used as nano storages after sputtering with a thin layer of metal.

## Acknowledgments

This work was supported by the National Natural Science Foundation of China (Grant Nos. 51572071, 21271067), and Program for Innovative Research Team in University (Grant No. IRT-1237), Ministry of Education, China.

## Notes and references

1 Q. Cao, H. S. Kim, N. Pimparkar, J. P. Kulkarni, C. Wang, M. Shim, K. Roy, M. A. Alam and J. A. Rogers, *Nature,* 2008, **454**, 495–500.
2 A. Thess, R. Lee, P. Nikolaev, H. J. Dai, P. Petit, J. Robert, C. H. Xu, Y.
H. Lee, S. G. Kim and R. E. Smalley, *Science*, 1996, **273**, 483–487.
3 N. Rouhi, D. Jain and P. Burke, *J. ACS. Nano*, 2011, **5**, 8471–8487.
4 C. Wang, J. Chien, K. Takei, T. Takahashi, J. Nah, A. M. Niknejad and A. Javey, *Nano Lett.*, 2012, **12**, 1527–1533.
5 M. E. Roberts, M. C. LeMieux and Z. Bao, *ACS. Nano*, 2009, **3**, 3287–3293.
6 R. J. Chen, H. C. Choi, S. Bangsaruntip, E. Yenilmez, X. Tang, Q. Wang, Y. L. Chang and H. *J.* Dai, *Am. Chem. Soc*., 2004, **126**, 1563 –1568.
7 D. Zhang, K. Ryu, X. Liu, E. Polikarpov, J. Ly, M. E. Tompson and C. Zhou, *Nano Lett*., 2006, **6**, 1880–1886.
8 L. Hu, D. S. Hecht and G. Gruner, *Chem. Rev*., 2010, **110**, 5790 –5844.

9 S. L. Hellstrom, H. W. Lee and Z. Bao, *ACS. Nano*, 2009, **3**, 1423 –1430.
10 N. Surugau and P. L. Urban, *J. Sep. Sci.,* 2009, **32**, 1889–1906.
11 M. J. Mendes, H. K. Schmidt and M. Pasquali, *J. Phys. Chem. B,* 2008, **112**, 7467–7477.
12 S. M. Tabakman, K. Welsher and G. Hong, *J. Phys. Chem. C,* 2010, **114**, 19569–19575.
13 Y. Feng, Y. Miyata and K. Matsuishi, *J. Phys. Chem. C*, 2011, **115**, 1752–1756.
14 A. M. Prantner, J. Chen and C. B. Murray, *Chemistry of Materials*, 2012, **24**, 4008–4010.
15 Y. Yamamoto, T. Fujigaya, Y. Niidomea and N. Nakashima, *Nanoscale*, 2010, **2**, 1767–1772.
16 G. S. Duesberg, W. Blau, H. J. Byrne, J. Muster, M. Burghard and S. Roth, *Synth. Metals,* 1999, **103**, 2484–2485.
17 H. Erik Haroz, G.Juan Duque, X. M. Tu, M. Zheng, R. Angela Hight Walker, H.Robert Hauge, K. Stephen Doorn and K. Junichiro, *Nanoscale*, 2013, **5**, 1411–1439.
18 M. Zheng, A. Jogota and E. D. Semke, *Nature Mater.,* 2003, **2**, 338–342.
19 M. Zheng, A. Jogota and E. Strano, *Science,* 2003, **302**, 1545–1548.
20 X. Tu, S. Manohar, A. Jagota and M. Zheng, *Nature,* 2009, **460**, 250–253.
21 H. Wang, J. Mei and P. Liu, *ACS. nano*, 2013, **7**, 2659–2668.
22 A. G. Nyankima, D. W.Horn and V. A. Davis, *ACS. Macro. Letters*, 2013, **3**, 77–79.
23 R. C. Chadwick, J. B. Grande and M. A. Brook, *Macromolecules*, 2014, **47**, 6527–6530.
24 K. Soai, T.Kawasaki and A. Matsumoto, *Accounts of chemical research*, 2014, **47**, 3643–3654.
25 H. Qui, Y. Maeda and T. Akasaka, *J. Am. Chem. Soc.,* 2009, **131**, 16529–16533.
26 C. M. Yang, J. S. Park and K. H. An, *J. Phys. Chem. B,* 2005, **109**, 19242–19248.
27 C. Bergeret, J. Cousseau, V. Fernandez, J. Y. Mevellec and S. Lefrant, *J. Phys. Chem. C ,* 2008, **112**, 16411–16416.
28 D. Nepal, S. Balasubramanian and A. L .Simonian, *Nano letters*, 2008, **8**, 1896–1901.
29 F. Bomboi, A. Bonincontro and C. La Mesa, *Journal of colloid and interface science*, 2011, **355**, 342–347.
30 Q. Hu, Y. Deng and Q. Yuan, *Journal of Polymer Science Part A*: *Polymer Chemistry*, 2014, **52**, 149–153.
31 T. Fukumaru, F. Toshimitsu, T. Fujigayaab and N. Nakashima, *Nanoscale*, 2014, **6**, 5879–5886.
32 W. Y. Xu, J. W. Zhao, L. Qian, X. Y. Han, L. zh. Wu, W. Ch. Wu, M. Sh. Song, L. Zhou, W. M. Su, Ch. Wang, Sh. H. Niea and Zh. Cui, *Nanoscale*, 2014, **6**, 1589–1595.
33 J. F. Ding, Zh. Li, F.Y. Cheng, G. Dubey, Sh. Zou, P. Finnie, A. Hrdina, L. Scoles, P. Gregory, T. Kingston and R. L. Patrick Malenfant, *Nanoscale*, 2014, **6**, 2328–2339.
34 F. Chen, B. Wang, Y. Chen and L. J. Li, *Nano Lett.*, 2007, **7**, 3013–3017.
35 W. Gomulya, G. D. Costanzo, E. J. F. de Carvalho, S. Z. Bisri, V. Derenskyi and M. Fritsch, *Adv. Mater.,* 2013*,* **25**, 2948–2956.
36 M. Tange, T. Okazaki and S. Iijima, *J. Am. Chem. Soc.,* 2011, **133**, 11908–11911.
37 H. Ozawa, T. Fujigaya, Y.Niidome and N. Nakashima, *Chem. Lett.,* 2011, **40**, 239– 241.
38 J. Gao, M. Kwak, J. Wildeman, A.Herrmann and M. A. Loi, *Carbon,* 2011, **49**, 333–338.
39 K. Akazaki, F. Toshimitsu, H. Ozawa, T. Fujigaya and N. Nakashima, *J. Am. Chem. Soc.*, 2012, **134**, 12700–12707.
40 P. Deria, C. D. Bargen, J. H. Olivier, A. S. Kumbhar, J. G. Saven and M. J. Therien, *J. Am. Chem. Soc.*, 2013, **135**, 16220–16234.
41 M. S. Dresselhaus, G. Dresselhaus, R. Saito and A. Jorio, *Phys. Rep.,* 2005, **95**, 217–403.
42 R. D. Miller and J. Michl, *Chemical Reviews*, 1989, **89**, 1359–1410.
43 A. R. Wolff, R. West, *Applied organometallic chemistry*, 1987, **1**, 7–14.
44 W. Chung, K. Nobusawa, H. Kamikubo, M. Kataoka, M. Fujiki and M. Naito, *J. Am. Chem. Soc*., 2013, **135**, 2374–2383.
45 M. Naito, K. Nobusawa, H. Onouchi, M.Nakamura, K. Yasui, A. Lkeda and M. Fujiki, *J. Am. Chem. Soc.*, 2008, **130**, 16697–16703.
46 R. H. Baughman, A. A. Zakhidov and W. A. de Heer, *Science,* 2002, **297**, 787–792.
47 J. Jiao, L.F. Dong, S. Foxlex, C. Mosher and D. W. Tuggle, *Microscopy and Microanalysis,* 2003, **9**, 516–521.
48 H. J. Dai, *Acc. Chem. Res.,* 2002, **35**, 1035–1044.
49 I. Szleifer and R. Yerushalmi-Rozen, *Polymer,* 2005*,* **46**, 7803–7818.
50 P. M. Ajayan and J. M. Tour, *Nature*, 2007, **447**, 1066–1068.
51 C. M. Kok and A. Rudin, *J. Appl. Polym. Sc*i., 1987, **27**, 353–362.
52 L. Liu, X. D. Li, X. Xing, Ch. Ch. Zhou and H.F. Hu, *Journal of Organometallic Chemistry,* 2008, **693**, 917–922; Z. F. Zhang, C. S. Scotto and R. M. Laine, *J. Mater. Chem.,* 1998, **8**, 2715; W. J. Pu, X. D. Li, G. Y. Li and T. J. Hu, *Polym. Bull.* 2015, **72**, 779-790; W. Zh. Wang, Q. Li. Fan, F. Cheng, P. Zhao, Wei Huang, *J. Polym. Sci.-A, Polym. Chem.*, 2006, **44**, 3513–3525.
53 T. Kawabe, M. Naito and M. Fujiki, *Macromolecules,* 2008, **41**, 1952–1960.
54 M. Naito and M. Fujiki, *Soft Matte*r, 2008, **4**, 211–223.
55 M. E. Itkis, D.E.Perea, S. Niyogi, S. M. Rickard and M. A. Haddon, *Nano Letters,* 2003, **3**, 309–314.
56 J. P Buisson, O. Chauvet, S. Lefrant, C. Stephan and J. M. Benoit, Mater. Res. Soc. Symp. Proc. 2001, 633, A14.12.1. (this reference is removed)
56 W. H. Yi, A. Maalkovskiy, Q. H. Chu, A. P. Sokolov, M. L. Colon M. Meador and Y. Pang, Wang, *J. Phys. Chem. C*, 2008, **112**, 12263–12269.
57 B. Gao, Y. Zhang and J. Zhang, *J. Phys. Chem. C*, 2008, **112**, 8319–8323.
58 K. E. Wise, C. Park, E. J. Siochi and J. S. Harrison, *Chem. Phys. Lett.* 2004, **391**, 207–211.
59 S. Suzuki, C. Bower, Y. Watanabe and O. Zhou, *Appl. Phys. Lett.*, 2000 **76**, 4007.
60 S. Kazaoui, N. Minami, N. Matsuda, H. Kataura and Y. Achiba, *Appl. Phys. Lett.,* 2001, **78**, 3433.
61 M. Naito, N. Saeki, M. Fujiki and A. Ohira, *Macromolecules*, 2007, **40**, 648–652.
62 D. Baskaran, J. W. Mays and M. S. Bratcher, *Chem. Mater.*, 2005, **17**, 3389–3397.



 

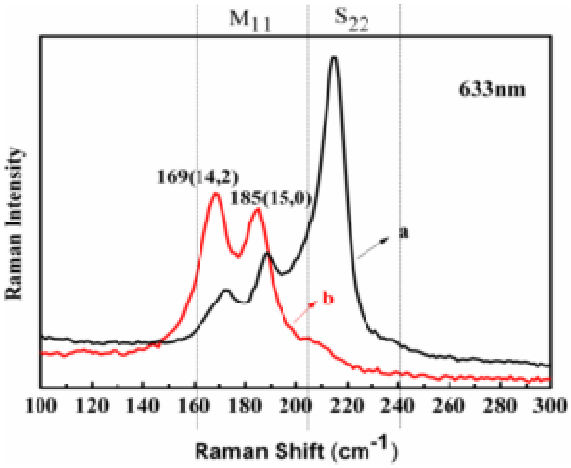


The arc-discharged metallic SWNTs are selectively extracted with a water soluble polymethyl(1-undecylic acidyl)silane by the formation of a charge donor-acceptor complex.